OPEN

Oncogene (2017) **36**, 1058–1068

www.nature.com/onc

ORIGINAL ARTICLE

Overexpression of *PDGFRA* cooperates with loss of *NF1* and *p53* to accelerate the molecular pathogenesis of malignant peripheral nerve sheath tumors

DH Ki[1], S He[1], S Rodig[2] and AT Look[1]

Malignant peripheral nerve sheath tumors (MPNSTs) are aggressive, frequently metastatic sarcomas that are associated with neurofibromatosis type 1 (NF1), a prominent inherited genetic disease in humans. Although loss of the *NF1* gene predisposes to MPNST induction, relatively long tumor latency in NF1 patients suggests that additional genetic or epigenetic abnormalities are needed for the development of these nerve sheath malignancies. To study the molecular pathways contributing to the formation of MPNSTs in NF1 patients, we used a zebrafish tumor model defined by *nf1* loss in a *p53*-deficient background together with the overexpression of either wild-type or constitutively activated *PDGFRA* (platelet-derived growth factor receptor-α) under control of the *sox10* neural crest-specific promoter. Here we demonstrate the accelerated onset and increased penetrance of MPNST formation in fish overexpressing both the wild-type and the mutant *PDGFRA* transgenes in cells of neural crest origin. Interestingly, overexpression of the wild-type *PDGFRA* was even more potent in promoting transformation than the mutant *PDGFRA*, which is important because ~78% of human MPNSTs have expression of wild-type *PDGFRA*, whereas only 5% harbor activating mutations of the gene encoding this receptor. Further analysis revealed the induction of cellular senescence in zebrafish embryos overexpressing mutant, but not wild-type, *PDGFRA*, suggesting a mechanism through which the oncogenic activity of the mutant receptor is tempered by the activation of premature cellular senescence in an *NF1*-deficient background. Taken together, our study suggests a model in which overexpression of wild-type *PDGFRA* associated with *NF1* deficiency leads to aberrant activation of downstream RAS signaling and thus contributes importantly to MPNST development—a prediction supported by the ability of the kinase inhibitor sunitinib alone and in combination with the MEK inhibitor trametinib to retard MPNST progression in transgenic fish overexpressing the wild-type receptor.

Oncogene (2017) **36,** 1058–1068; doi:10.1038/onc.2016.269; published online 1 August 2016

INTRODUCTION

Malignant peripheral nerve sheath tumors (MPNSTs) are aggressive and often metastatic soft-tissue sarcomas that occur most frequently in children and young adults with neurofibromatosis type 1 (NF1).[1] Indeed, about half of all MPNSTs are diagnosed in NF1 patients, and MPNSTs represent one of the most common causes of death in patients who are haploinsufficient for this gene.[2] These nerve sheath tumors are thought to arise from cells derived from the neural crest, including progenitors of Schwann cells and perineural cells, which have somatically lost the function of the remaining *NF1* allele.[3] The prognosis of patients with MPNSTs is very poor, with a high recurrence rate after surgical resection (~40%).[4,5] Currently, complete surgical excision is the only curative therapy for these tumors, but unfortunately they are often not completely resectable. The available chemotherapy regimens are for the most part ineffective, and are often associated with significant toxicity that can severely reduce quality of life. Therefore, improved understanding of MPNST pathogenesis and the identification of new molecular pathways on which these tumors are dependent is urgently needed to improve treatment outcome in NF1 patients who develop malignant nerve sheath tumors. Hopefully, new insights into pathogenesis will implicate potential therapeutic targets for the development of small-molecule drugs with more potent and specific antitumor activity.

Patients with NF1 have only one functional copy of the *NF1* gene, which encodes neurofibromin, a protein of more than 2800 amino acids.[6] Neurofibromin contains a small region of homology to the RAS GAP protein and is capable of downregulating RAS activity by accelerating the hydrolysis of GTP-bound RAS to its inactive GDP-bound form.[7] Thus, when the remaining functional allele of *NF1* is lost somatically in nonmyelinating Schwann cell progenitors, the NF1-null progeny acquire aberrant growth properties leading to benign neurofibromas.[8,9] These benign neurofibromas can occur in association with cutaneous nerves in the form of dermal neurofibromas, often causing cosmetic disfiguration. Plexiform neurofibromas are a more serious second type of neurofibroma that form in association with more internal nerve bundles. In this type of neurofibroma, other cell types are recruited, including fibroblasts, perineural cells, endothelial cells and mast cells. Plexiform neurofibromas invade soft-tissue structures and bone, often causing significant functional impairment depending on their location.[10] Even though plexiform neurofibromas are benign tumors, they are often unresectable

[1]Department of Pediatric Oncology, Harvard Medical School/Dana-Farber Cancer Institute, Children's Hospital Boston, Boston, MA, USA and [2]Brigham and Women's Hospital, Boston, MA, USA. Correspondence: Professor AT Look, Department of Pediatric Oncology, Harvard Medical School/Dana-Farber Cancer Institute, Children's Hospital Boston, 450 Brookline Avenue, Mayer 630, Boston, MA 02115, USA.
E-mail: Thomas_look@dfci.harvard.edu
Received 21 January 2016; revised 9 June 2016; accepted 16 June 2016; published online 1 August 2016

because they involve multiple layers of tissues with essential functions. About 10% of plexiform neurofibromas undergo malignant transformation into MPNSTs,[11] often arising from cells with the additional acquired loss of the *CDKN2A* or *TP53* tumor suppressor genes.[12]

The absence or latency of MPNST development in many NF1 patients suggests that additional gene mutations are needed to induce tumorigenesis. One promising candidate is platelet-derived growth factor receptor-α (*PDGFRA*), a receptor tyrosine kinase (RTK). Overexpression and chromosomal amplification of the *PDGFRA* gene have been reported in MPNSTs,[13,14] and this gene was one of the most overexpressed in an analysis of paired benign plexiform neurofibromas and MPNSTs,[15] suggesting that this RTK may be upregulated as part of the benign-to-malignant tumor transition. Moreover, *PDGFRA* is frequently active and phosphorylated in MPNSTs from patients.[16,17] Both *PDGFRA* and its ligand, PDGF-A, are overexpressed together in human MPNST cells,[16] suggesting that PDGF-A ligand acts in an autocrine manner in human MPNSTs to support growth. Paracrine stimulation also supports MPNST growth because Schwann cells derived from $nf1^{-/-}$ mice express growth factor ligands such as PDGF-B, unlike those derived from $nf1^{+/+}$ mice.[18] Overall, both autocrine and paracrine activation of the PDGF receptor seem to be responsible for accelerating human MPNST formation. Taken together, these findings justify a more comprehensive investigation of the role of *PDGFRA* in the molecular pathogenesis of MPNSTs in patients with loss of the *NF1* gene. This imperative gains impetus from reports that RTK inhibitors targeting PDGFRA decrease the growth and invasion rates of MPNST cell lines.[16,19]

We previously reported that zebrafish with loss-of-function mutations of *p53* develop MPNST,[20] reiterating the observation of *p53* loss in human MPNST.[21] Thus, to discover the molecular pathways contributing to the formation of MPNSTs in NF1 patients, we generated an NF1 mutant zebrafish model and used it to demonstrate that a combination of *nf1* loss and *p53* deficiency potentiates the penetrance and onset of MPNSTs.[22] To better understand the molecular and cellular determinants of NF1-associated MPNST pathogenesis *in vivo*, we established stable transgenic lines with overexpression of both wild-type and constitutively active mutant of human *PDGFRA*, using the MPNST-prone zebrafish line with loss of both *p53* and *nf1*. We report here that MPNST onset is accelerated by *PDGFRA* overexpression. Interestingly, overexpression of wild-type *PDGFRA* was more active in accelerating MPNST initiation than was mutationally activated *PDGFRA* in our transgenic zebrafish model, possibly because mutationally active PDGFRA induces senescence in *nf1/p53* compound mutant cells. Thus, our study implicates overexpression of wild-type *PDGFRA* as a key driver in MPNST, which is important because wild-type *PDGFRA* is frequently documented in human MPNST, whereas mutational activation of the gene is rare. This is a key consideration when implementing targeted therapy, because it indicates that PDGFRA inhibitors are likely to have antiproliferative activity in the large subset of MPNSTs with overexpression of wild-type *PDGFRA*.

RESULTS

I-SceI meganuclease-mediated *PDGFRA* transgenesis in *nf1*- and *p53*-deficient fish

To understand the role of *PDGFRA* in MPNST pathogenesis, we cloned the cDNA encoding either wild-type or constitutively activated human *PDGFRA* (exons 8 and 9 deleted)[23] under control of the zebrafish *sox10* neural crest-specific promoter (Figure 1a). A *sox10:mCherry* cDNA construct was coinjected with each *sox10:PDGFR* construct into $nf1a^{+/-}$; $nf1b^{-/-}$; $p53^{m/m}$ zebrafish, based on studies showing that three separate transgene constructs will cointegrate into the host genome after coinjection into the one-cell-stage zebrafish embryo.[24] Hence, the expression of *mCherry* serves as a marker for the coexpression of *PDGFRA* in tissues of the mosaic primary injected animals.

At maturity 3 months after injection, the primary injected animals were outbred to establish stable transgenic lines with overexpression of either wild-type or mutant *PDGFRA* in $nf1a^{+/-}$; $nf1b^{-/-}$; $p53^{m/m}$ zebrafish. To confirm the presence of the human *PDGFRA* gene in zebrafish DNA, we performed PCR with the extracted total DNA from individual embryos of the stable lines, detecting the human wild-type *PDGFRA* (740 bp) and mutant (497 bp) PCR bands (Figures 1b and c). In the stable transgenic lines, the mCherry fluorescence, driven by the *sox10* promoter, is expressed in cells of neural crest origin during early embryogenesis (Figures 1d and e).[25]

Hyperplasia of oligodendrocyte progenitor cells (OPCs) and decreased lateral stripe melanophores have been reported in our previous study with *nf1* mutant zebrafish.[22] We examined whether PDGFRA overexpression affects these cells (Supplementary Figure S1). In these results, 6 days post fertilization (d.p.f.) embryos from both wild-type and mutant *PDGFRA* transgenic lines demonstrated increased numbers of *sox10:mCherry*-positive OPCs in the spinal cord. Embryos transgenic for mutant *PDGFRA* had the most marked increase in OPCs, with approximately twice the number of *sox10:mCherry*-positive OPCs compared with the *mCherry* control transgenic larvae in the $nf1a^{+/+}$; $nf1b^{-/-}$; $p53^{m/m}$ background. Decreased lateral stripe melanophores were identified in our current study in the $nf1a^{+/+}$; $nf1b^{-/-}$; $p53^{m/m}$ background, similar to results we reported previously,[22] and there was no detectable difference among the *mCherry* control, wild-type and mutant *PDGFRA* transgenic zebrafish. We did not observe any additional developmental defects in the *PDGFRA* transgenic zebrafish embryos.

Both wild-type and constitutively activated mutant forms of PDGFRA accelerate MPNST tumorigenicity in *nf1*- and *p53*-deficient fish

We performed tumor watches using both mosaic primary injected fish and established stable transgenic lines, and found that both wild-type and constitutively activated mutant *PDGFRA* transgenes accelerated MPNST tumorigenesis and increased tumor penetrance in $nf1a^{+/-}$; $nf1b^{-/-}$; $p53^{m/m}$ zebrafish (Figures 2a and b). In primary injectants, both wild-type and mutant *PDGFRA*-injected zebrafish developed mCherry-positive tumors much earlier and more frequently than in *mCherry* control fish (Figure 2a). In *PDGFRA* mutant injectants, tumor onset began at 20 weeks post fertilization (w.p.f.), whereas in those *PDGFRA* injected with wild-type, they began to form at 25 w.p.f., and mCherry-only control transgenic fish developed tumors from 31 weeks. Interestingly, both wild-type and *PDGFRA* mutant injectants showed higher penetrance rates than did *mCherry* control zebrafish (71.4% and 55.6% vs 27.3% at 40 w.p.f). These results in the primary injectants show that both wild-type and constitutively activated *PDGFRA* overexpression cooperate with loss of *nf1* and *p53* function to accelerate the onset and increase the penetrance of tumor formation.

In these stable transgenic lines derived from outbreeding the primary injectants, including *Tg(*$nf1a^{+/-}$; $nf1b^{-/-}$; $p53^{m/m}$*; sox10:wild-type PDGFRA; sox10:mCherry), Tg(*$nf1a^{+/-}$; $nf1b^{-/-}$; $p53^{m/m}$*; sox10:PDGFRA* mutant; *sox10:mCherry),* and *Tg(*$nf1a^{+/-}$; $nf1b^{-/-}$; $p53^{m/m}$*; sox10:mCherry)* also developed tumors (Figure 2b). In the stable fish lines, the tumor onset times and penetrance patterns associated with both the wild-type and mutant forms of *PDGFRA* were similar to those of the mosaic *PDGFRA* wild-type and mutant injectants, reflecting a faster growth rate of tumors overexpressing wild-type compared with constitutively activated *PDGFRA*. Tumors arose at 18 w.p.f. in the wild-type *PDGFRA*-overexpressing fish, with 89.3% of this group developing MPNSTs by 30 w.p.f.

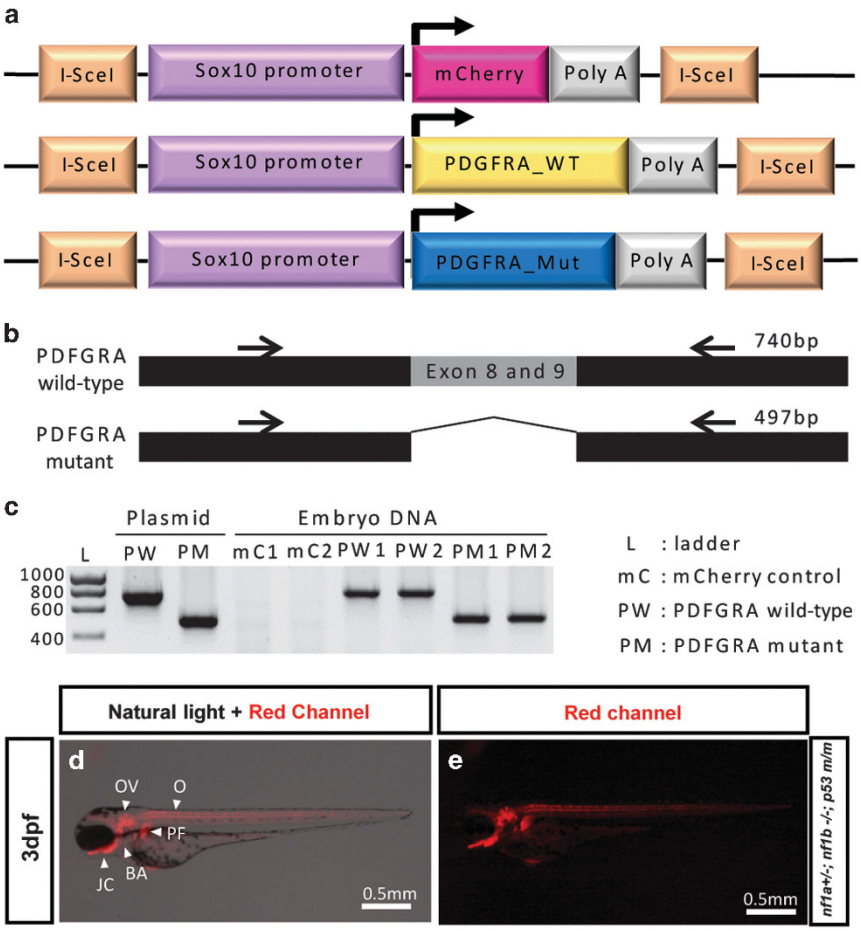

Figure 1. I-SceI meganuclease-mediated human *PDGFRA* transgenesis in *nf1*- and *p53*-deficient fish. (**a**) Schematic diagram of the DNA constructs used to generate transgenic *sox10:mCherry*, *sox10*:wild-type (WT) and constitutively activated (Mut) *PDGFRAs* zebrafish. I-SceI denotes the I-SceI meganuclease target sequence. (**b**) Schematic diagram of PCR target of human wild type and constitutively activated mutant *PDGFRA* (Δ exons 8 and 9) for genotyping. Black arrows represent primer target sites for PCR. (**c**) PDGFRA wild-type and mutant DNA sequences were detected in genomic DNA of the transgenic zebrafish embryos. Human *PDGFRA* sequences were confirmed with embryonic DNA of two separate transgenic lines (mC1 and mC2, PW1 and PW2 and PM1 and PM2). Each amplified PCR band of *PDGFRA* wild type and mutant had sizes of 740 and 497 bp, respectively. Injected plasmids for transgenesis were used as the positive control. (**d** and **e**) *Sox10* promoter driving *mCherry* is expressed in cells of neural crest origin during early embryogenesis. *Tg* (*nf1a*$^{+/-}$; *nf1b*$^{-/-}$; *p53*$^{m/m}$; *sox10:mCherry*) zebrafish embryo at 3 d.p.f. showed mCherry expression throughout otic vesicle (OV), branchial arches (BA), oligodendrocytes (O), jaw cartilage (JC) and pectoral fins (PF).

Transgenic *PDGFRA* mutant zebrafish began to show tumors by 20 w.p.f., with 48.3% developing tumors by 30 w.p.f. This contrasts with the lack of onset of tumors in the *mCherry* control zebrafish until 24 w.p.f., and a tumor penetrance rate of 22.8% at 30 w.p.f.

These findings reinforce the status of *PDGFRA* as a key driver of tumorigenesis in MPNST. The faster development of tumors in *PDGFRA* wild-type overexpressors compared with *PDGFRA* mutant fish was surprising, likely reflecting optimal *PDGFRA* tyrosine kinase activity when the wild-type receptor is overexpressed as opposed to constitutive activation of the *PDGFRA* gene. Apparently, the constitutively activated mutant *PDGFRA* is so active in an *nf1/p53*-deficient background that it actually reduces tumor cell growth by inducing cellular senescence (see below and Figures 4d–l). This interpretation also agrees with reports that human MPNST samples often show high levels of PDGFRA expression without any mutation in the PDGFRA coding sequence.[16]

The *sox10* promoter is highly expressed in MPNST,[26,27] and thus transgenic *sox10:mCherry* (Figures 2c and d), *sox10:mcherry/PDGFRA* wild-type (Figures 2e and f) and *sox10:mcherry/PDGFRA* mutant (Figures 2g and h) zebrafish developed tumors with strong mCherry expression. Evaluation of the induced zebrafish MPNSTs for PDGFRA expression demonstrated expression of human PDGFRAs in protein lysates prepared from tumors of fish transgenic for wild-type and mutant *PDGFRAs* (Figure 2i). Their phosphorylated (active) forms were also detected. Interestingly, a phosphoprotein with the same mobility as human PDGFRA was detected in *mCherry* control tumor lysates, suggesting that the endogenous zebrafish receptor tyrosine kinase is activated during the molecular pathogenesis of zebrafish MPNST.

PDGFRA-induced zebrafish MPNSTs exhibit similar histology to that of human MPNSTs

To examine the histology of the induced tumors in our transgenic zebrafish, we performed hematoxylin and eosin (H&E) staining. The results were consistent with the diagnostic histologic features of human MPNST: spindle-shaped cells with long serpentine-like nuclei that stack into short fascicles, typically organized into whorls (Figures 3a–c).

We also examined the expression of two neural crest cell lineage markers, S100 and Sox10, in our zebrafish MPNST tumors, as these are used diagnostically to distinguish human MPNST from other types of solid tumors.[26,27] Both S100 (Figures 3d–f) and

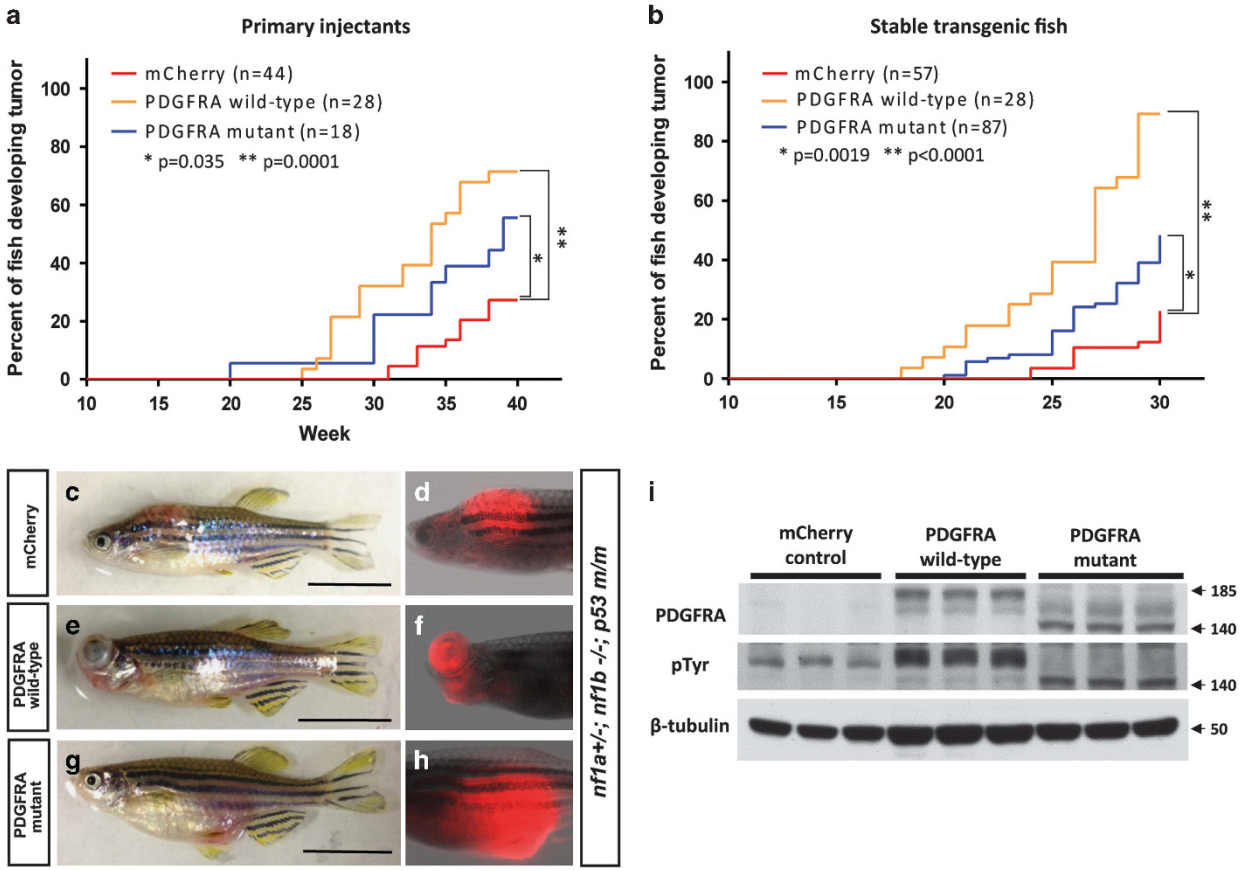

Figure 2. Both wild-type and constitutively activated mutant forms of PDGFRA accelerate MPNST tumorigenicity in *nf1*- and *p53*-deficient fish. (**a** and **b**) Kaplan–Meier analysis of tumorigenesis in fish with either mosaic or stable expression of the *PDGFRA* transgene. Onset of MPNSTs in *nf1*- and *p53*-deficient zebrafish ($nf1a^{+/-}$; $nf1b^{-/-}$; $p53^{m/m}$) injected with the following DNA constructs: (1) *sox10:mCherry* alone (mCherry, red); (2) *sox10:PDGFRA* wild-type and *sox10:mCherry* (*PDGFRA* wild-type, yellow); or (3) *sox10:PDGFRA* mutant and *sox10:mCherry* (*PDGFRA* mutant, blue). Note that wild-type *PDGFRA* overexpression accelerated the onset of MPNSTs more rapidly than constitutively activated mutant *PDGFRA*. (**c–h**) Representative images of the *sox10* promoter driving mCherry-positive tumors under different conditions. Transgenic *sox10:mCherry* (**c** and **d**), *sox10:mcherry/PDGFRA* wild-type (**e** and **f**) and *sox10:mCherry/PDGFRA* CA mutant (**g** and **h**) in the $nf1a^{+/-}$; $nf1b^{-/-}$; $p53^{m/m}$ background induced tumors that strongly expressed mCherry protein (>30 w.p.f., scale bar = 10 mm). (**i**) Western blot analysis for PDGFRA in protein lysates prepared from tumors of *mCherry* control, *PDGFRA* wild-type and *PDGFRA* mutant fish. *PDGFRA* wild-type, mutant and their phosphorylated (active) forms were detected. β-Tubulin was used an internal control for equal loading. Arrow denotes protein size (kDa).

Sox10 (Figures 3g–i) were expressed by tumor cells in samples of tumors arising in each of our transgenic lines. S100 is localized in the cell membrane and nucleus, whereas Sox10 is only detected in the nucleus. The histopathologic features were identical to those in MPNSTs arising in the $nf1a^{+/-}$; $nf1b^{-/-}$; $p53^{m/m}$ line expressing *mCherry*, and in fish with the same background mutations but expressing the wild-type or mutant *PDGFRA* transgene.

Additionally, we performed immunohistochemical staining to identify which cells and tissues expressed PDGFRA in adult zebrafish (Supplementary Figure S2). Endogenous PDGFRA was expressed in many adult zebrafish tissues such as brain, gill and oocytes. MPNST tumor cells from *sox10:mCherry*, *wild-type* and *mutant PDGFRA* zebrafish lines each also expressed detectable PDGFRA. The mutant PDGFRA protein is predominately expressed in the cytosol, as noted previously.[23]

Overexpression of the *PDGFRA* wild-type gene activates AKT and ERK at levels optimal for tumorigenicity

We expected that PDGFRA overexpression and activation of its tyrosine kinase domain would activate phosphatidylinositol-4,5-bisphosphate 3 kinase and Ras downstream signals in neural crest origin cells, and consequently would accelerate MPNST tumorigenicity. To test this prediction, we performed western blot analysis for AKT and ERK1/2 activation in protein lysates prepared from tumors of *mCherry* control, wild-type *PDGFRA* and *PDGFRA* mutant fish. Both AKT and ERK1/2 were phosphorylated in all types of primary MPNST lysates (Figure 4a). However, the phospho-AKT and phospho-ERK1/2 levels in the lysate of the *PDGFRA* mutant tumor were higher compared with those of the *mCherry* control and *PDGFRA* wild-type tumors. The mean values for the phosphorylated (p)-AKT/AKT and p-ERK/ERK ratios in the *PDGFRA* mutant were 3.68- and 3.10-fold higher, respectively, compared with that for the *mCherry* control (Figures 4b and c), whereas the phosphorylation levels of AKT and ERK1/2 in the lysates of *mCherry* and *PDGFRA* wild-type tumors were similar. Because the *PDGFRA* mutant tumors grow more slowly than *PDGFRA* wild-type tumors, our findings suggest that the wild-type *PDGFRA* may activate Ras downstream signals at levels optimal for MPNST tumorigenicity, whereas the *PDGFRA* mutant may transmit a stronger than optimal signal.

PDGFRA mutant overexpressors showed senescence-associated β-galactosidase activity

We hypothesized that excessive activation of Ras signaling by the mutant *PDGFRA* receptor might induce senescence in a subset of the MPNST cells, thus delaying the initiation of MPNST

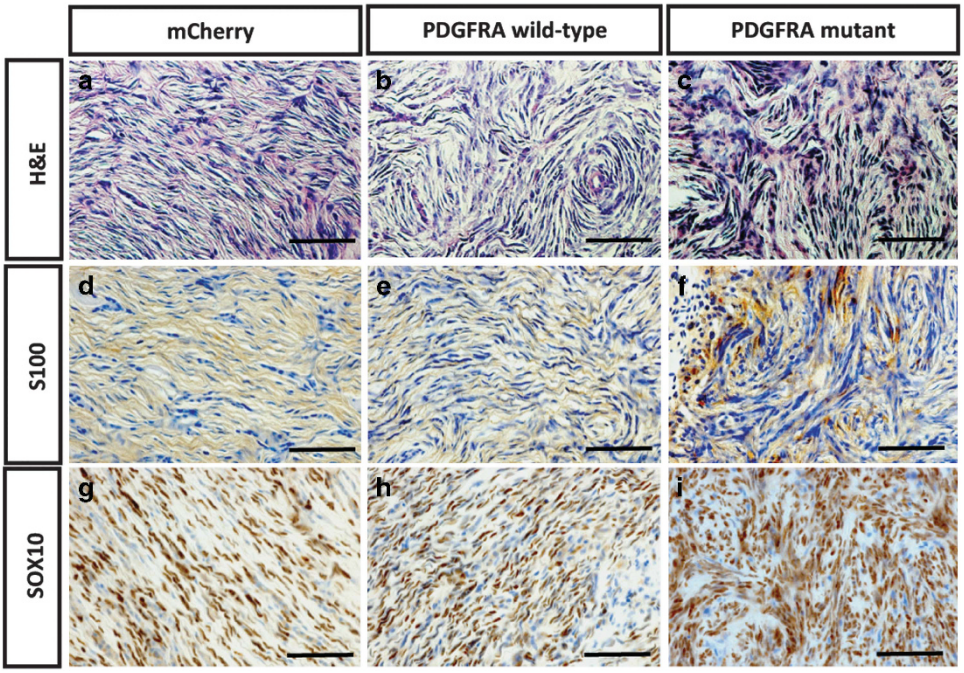

Figure 3. PDGFRA-induced zebrafish MPNST tumors exhibit similar histology to that of human MPNSTs. (**a–c**) The histopathology after H&E staining of the zebrafish MPNSTs was identical in the *nf1a*$^{+/-}$; *nf1b*$^{-/-}$; *p53m/m* zebrafish when either *PDGFRA* wild-type or mutant proteins were overexpressed. In each genotype, the zebrafish MPNST histopathology was very similar to that of human MPNSTs. The zebrafish MPNSTs comprise spindle cells that stack into short fascicles, typically with a whirling organization pattern. MPNST cells have long serpentine-like nuclei and are spindle-shaped. (**d–i**) Markers of cells of neural crest origin were expressed by the zebrafish MPNST tumors, such as S100 (**d–f**) and Sox10 (**g–i**). S100 was detected in the cell membrane and nucleus, whereas Sox10 was detected in the nucleus. Scale bar = 200 μm.

tumorigenesis during development. To test this hypothesis, we checked senescence-associated β-galactosidase activity of the cells in our zebrafish model at 4 d.p.f. In this result, the *PDGFRA* mutant overexpressors in *nf1*- and *p53*-deficient background showed higher levels senescence-associated β-galactosidase activity than did the wild-type *PDGFRA* overexpressors or controls (Figures 4d, g and j). In transverse sections of the embryos, senescence-associated β-galactosidase-stained cells coincided with or were adjacent to Sox10-expressing mCherry-positive cells within the ventral neural tube of transgenic fish overexpressing the PDGFRA mutant cDNA (Figures 4e, f, h, i, k and l). This result suggests that overexpression of the *PDGFRA* mutant in cells of neural crest origin may induce senescence through hyperstimulation of Ras signaling. Senescent cells become postmitotic, so this process would delay the onset and retard the growth of MPNST tumors in the *PDGFRA* mutant animals.

Furthermore, to detect senescence in MPNSTs derived from wild-type or mutant *PDGFRA* transgenic zebrafish, we performed β-galactosidase staining of the cryosectioned tumor tissues. We also examined fibrosis in both groups of tumors with the trichrome stain and antibodies to detect collagen I expression. Additionally, CD31 expression levels were assessed in the cryosectioned tumor tissues. In these experiments, we did not observe any differences in senescence, fibrosis or vascularity among the transgenic and *mCherry* control tumors (Supplementary Figures S4).

Sunitinib retards primary MPNST progression in wild-type *PDGFRA* transgenic fish

To test whether inhibition of PDGFRA and other tyrosine kinase receptors would affect tumor cell growth and survival, we treated *sox10:PDGFRA* wild-type transgenic MPNST fish with the RTK inhibitor, sunitinib for 10 days (2 μM sunitinib or dimethyl sulfoxide (DMSO) in fish water). In the adults, the drug was effectively absorbed by the gills and transported to the tumor cells and normal cells through the blood. Comparison of mCherry expression by the tumor pretreatment and post-treatment tumor area indicated retarded tumor cell growth in the sunitinib-treated fish (Figures 5a–l). Sunitinib-treated *PDGFRA* wild-type transgenic fish showed an average tumor growth of 11% over 10 days, compared with 300% growth over 10 days in the DMSO-treated fish (Figure 5m).

Sunitinib promotes apoptosis of MPNST cells of *PDGFRA* wild-type transgenic fish

To study how sunitinib treatment leads to tumor shrinkage, we first examined the histopathology of the DMSO- or sunitinib-treated fish after H&E staining (Figures 6a–h). The sunitinib-treated tumors showed areas of necrosis (Figures 6c, d and g, h), with the necrotic centers surrounded by MPNST cells, whereas areas of necrosis were not detected in the DMSO control tumors (Figures 6a, b and e, f). We also performed proliferating cell nuclear antigen and cleaved caspase-3 immunostaining to assess proliferation and apoptosis, respectively (Figures 6i–l and m–p). Positive staining for proliferating cell nuclear antigen was observed in both the DMSO- and the sunitinib-treated MPNSTs at about the same levels, with the positive immunostaining of cleaved caspase-3 observed only in the cell nuclei of tumors in the sunitinib-treated MPNSTs. This result suggests that sunitinib retards the progression of primary MPNSTs by inducing apoptotic cell death rather than by simply inhibiting cell proliferation.

Sunitinib activity is enhanced when given in combination with the MEK inhibitor trametinib in an *in vivo* assay using implanted zebrafish MPNST cells

MEK inhibitors have been reported to show activity against human MPNST cell lines.[28] To test whether sunitinib activity is enhanced

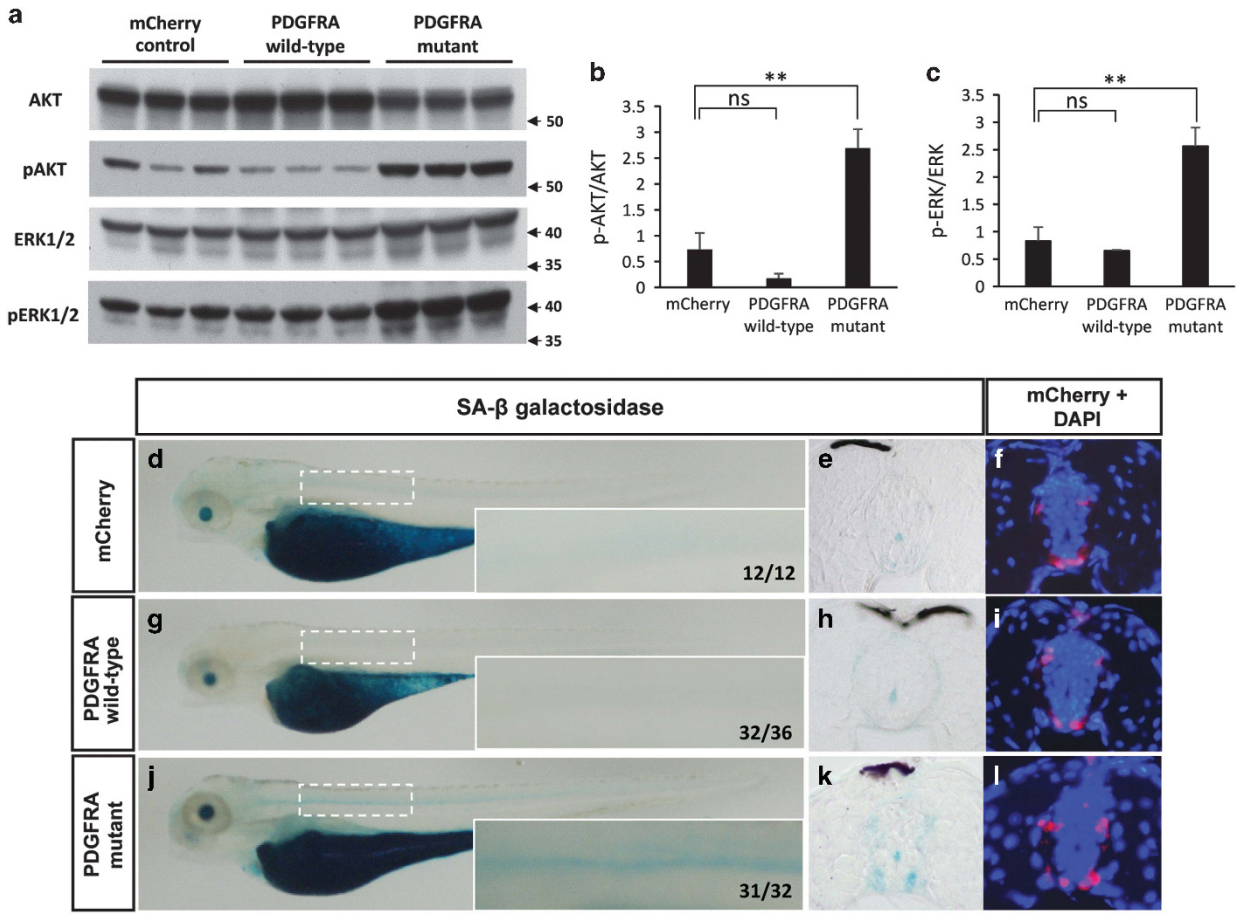

Figure 4. Overexpression of the *PDGFRA* wild-type gene activates AKT and ERK at levels optimal for tumorigenicity. (**a**) Western blot analysis for AKT and ERK1/2 activation in protein lysates prepared from tumors of *mCherry* control, *PDGFRA* wild-type, and *PDGFRA* mutant fish. Similar levels of p-AKT and p-ERK1/2 were detected in *PDGFRA* wild-type tumors as compared with *mCherry* control tumors; however, tumors induced by the *PDGFRA* mutant showed increased levels of p-AKT and p-ERK1/2. Proteins were detected by stripping the membrane and reprobing. Arrows denote protein size (kDa). (**b** and **c**) Statistical analysis of mean ± s.d. of p-AKT/total AKT and p-ERK/total AKT using ImageJ. Asterisks indicate statistical significance (**$P < 0.005$). (**d**, **g** and **j**) Representative images of SA-β galactosidase-stained transgenic fish embryos of *mCherry* control ($n = 12$), *PDGFRA* wild-type ($n = 36$) and *PDGFRA* mutant ($n = 32$) in the *nf1a*$^{+/-}$; *nf1b*$^{-/-}$; *p53m/m* background at 4 d.p.f. The boxed areas were magnified at the right bottom corner of each panel. (**e, h** and **k**) Transverse cryosections through the spinal cord of embryos at 4 d.p.f., with mCherry and DAPI (4',6-diamidino-2-phenylindole; **f**, **i** and **l**).

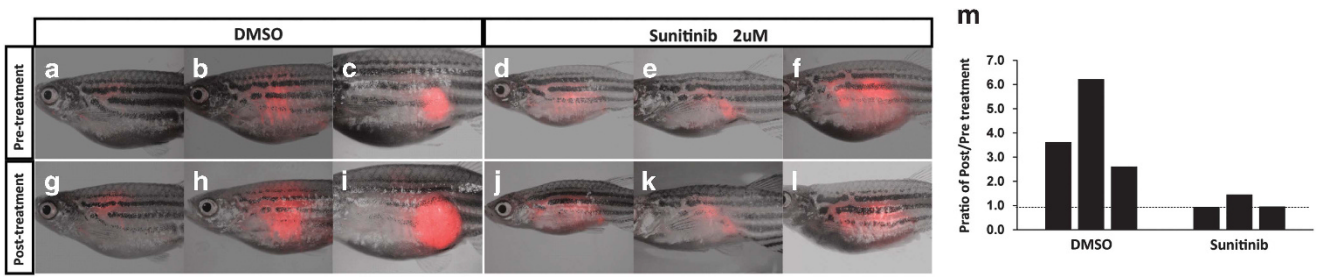

Figure 5. Sunitinib retards the progression of primary MPNSTs in transgenic fish with wild-type *PDGFRA*. (**a–f**) Images of *Tg* (*sox10:PDGFRA* wild-type; *sox10:mCherry*; *nf1a*$^{+/-}$; *nf1b*$^{-/-}$; *p53*$^{m/m}$) zebrafish with primary MPNSTs before drug treatment. mCherry driven by the *sox10* promoter is expressed by the tumor cells. Fish with MPNSTs were incubated in 2 μM of sunitinib ($n = 3$) or DMSO ($n = 3$) in the fish water for 10 days. (**g–l**) After drug treatment, tumor images were taken under the same condition as before treatment. (**m**) Comparison of cross-sectional areas of MPNSTs after sunitinib treatment and the DMSO control shows that the tumors increase in size when treated with the DMSO vehicle, and that this growth appears to be retarded by sunitinib treatment ($P < 0.05$).

when given in combination with a MEK inhibitor *in vivo*, we used the Food and Drug Administration-approved MEK inhibitor trametinib for this experiment. We transplanted primary MPNST cells of wild-type *PDGFRA* transgenic fish in the *nf1a*$^{+/-}$; *nf1b*$^{-/-}$; *p53*$^{m/m}$ background into 2-day-old embryos. Because thymocytes have not begun to develop at this stage of embryogenesis, injected tumor cells from a donor fish with MPNST will expand in Casper recipient zebrafish embryos without rejection, even up to 8 weeks of age (Figures 7a–f). After cell implantation at 2 d.p.f., embryos were incubated for 24 h before

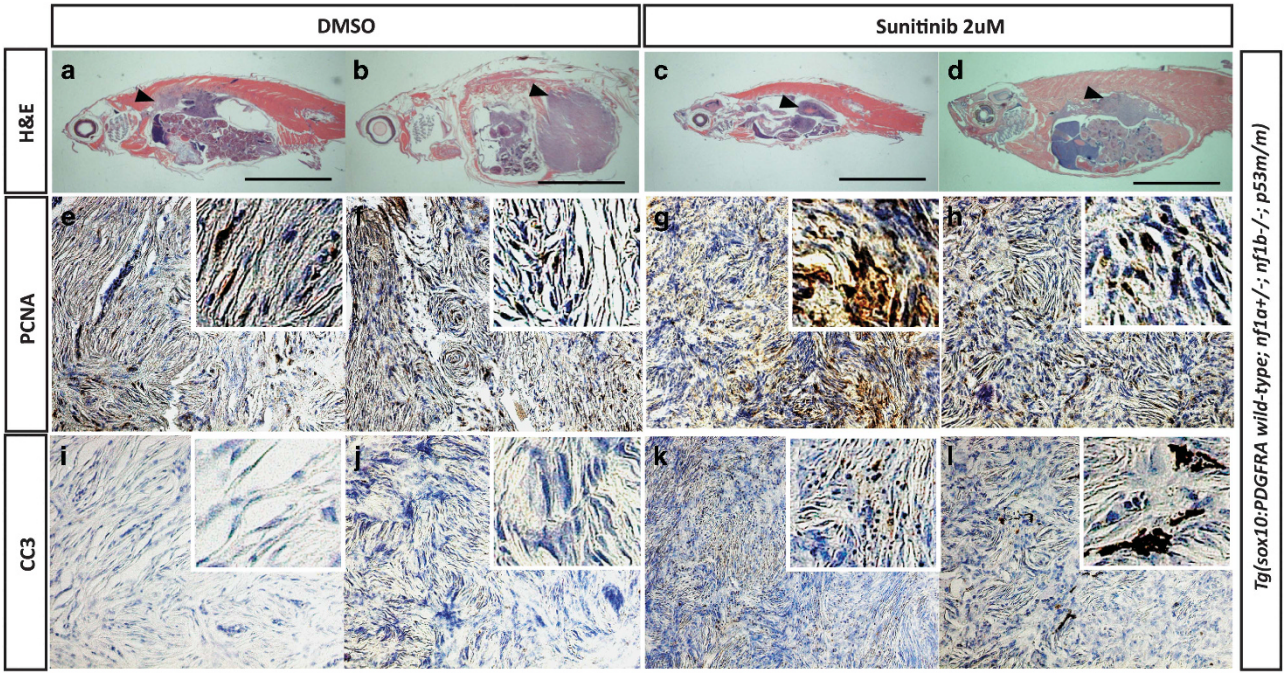

Figure 6. Sunitinib promotes apoptosis of primary MPNST progression in transgenic fish expressing wild-type *PDGFRA*. (**a–d**) Histopathology after H&E staining of the DMSO- (**a** and **b**) or sunitinib- (**c** and **d**) treated MPNSTs. Black arrowheads show areas of MPNSTs (black scale bar = 5 mm). Proliferating cell nuclear antigen (**e–h**) and cleaved caspase-3 (**i–l**) stains of each condition for proliferation and apoptosis analysis, respectively. The right upper corner of each panel shows magnified stained areas.

drug treatment. Successfully implanted embryos were incubated with drugs for 3 days (Figure 7g). Both trametinib and sunitinib alone were able to significantly suppress MPNST cell growth compared with the DMSO control group. Our results show marked potentiation of cell killing in embryos receiving sunitinib plus trametinib, compared with sunitinib alone (Figures 7i–n). These results support the concept that RTK-RAS-MAPK signaling is hyperactivated in nf1-deficient zebrafish, and thus direct inhibition of MEK is able to synergize with the RTK inhibitory activity of sunitinib to improve the response of MPNST tumor cells *in vivo*.

DISCUSSION

Here we compare the consequences of overexpression of wild-type and mutant *PDGFRA* on the onset and penetrance of MPNSTs arising in our *nf1*- and *p53*-deficient zebrafish model. Relying on the *sox10* promoter to overexpress wild-type and mutant *PDGFRA* in cells of neural crest origin, we demonstrate that PDGFRA overexpression accelerates MPNST tumorigenicity in zebrafish. Surprisingly, overexpression of wild-type *PDGFRA* was even more active in promoting the development of MPNST than was overexpression of a constitutively activated mutant *PDGFRA* in the *nf1*- and *p53*- deficient background (see Figures 2a and b). This observation has considerable clinical importance, because *PDGFRA* is frequently expressed at high levels in primary human MPNSTs, but it is only rarely mutated in these tumors.[16] Our results implicate this high level of expression of the wild-type receptor in pathogenesis, which is difficult to infer in the absence of evidence from an animal model. In addition, our studies show that inhibition of the tyrosine kinase activity with sunitinib in tumors arising in animals transgenic for the wild-type receptor is active in inducing apoptosis and delaying tumor growth, suggesting dependence on this pathway for maintenance as well as for the initiation of MPNST, and suggesting a role for this drug in the management of tumors that overexpress the wild-type receptor.

Mutational activation of *PDGFRA* is common in many types of cancers, such as gastrointestinal stromal tumors,[29,30] myeloproliferative malignancies associated with hypereosinophilia[31–33] and glioblastoma.[23,34] Most of these mutations act by promoting dimerization of the receptors in the absence of ligand, resulting in activation of the receptor's intracellular tyrosine kinase domain.[35] However, *PDGFRA* mutations in human MPNSTs are relatively rare, despite evidence of high levels of expression of the receptor and increased DNA copy number for the region surrounding the location of the gene.[14,16] Our studies suggest that this is because overexpression of constitutively active mutant PDGFRA induces excessive levels of oncogenic stress in NF1-deficient Schwann cell precursors, resulting in premature cell senescence.[36–38] It would appear that high levels of wild-type *PDGFRA* expression are sufficient to promote dimerization of a subset of the receptors on the cell surface by mass action, and that this relatively modest level of tyrosine kinase signaling is optimal to promote malignant transformation of NF1 defiant Schwann cells.

A second possibility is that other oncogenic signals activated by wild-type *PDGFRA* may be involved in MPNST development. Clarke *et al.*[23] reported that wild-type *PDGFRA* and exon 8- and 9-deleted mutant forms were differently localized in cells, with the mutants mainly expressed in cell cytosol and the wild-type form in the cell membrane. Because many cell signals are precisely regulated through receptors and transporters on the cell membrane, changes in the localization of PDGFRA may affect the outcome of RTK-related cell signaling such as calcium regulation, endocytosis and focal adhesion.[39–41] Thus, signaling through the correctly localized wild-type *PDGFRA* may produce optimal signals for MPNST initiation.

The Sox10 protein is a neural crest transcription factor that is active in the differentiation of Schwann cell precursors.[42] In our previous study, we confirmed that GFP driven by the *sox10* promoter is strongly expressed in OPCs and Schwann cells,[22] so that this promoter is ideal for driving gene expression in this lineage. Moreover, the tumor cells themselves express Sox10

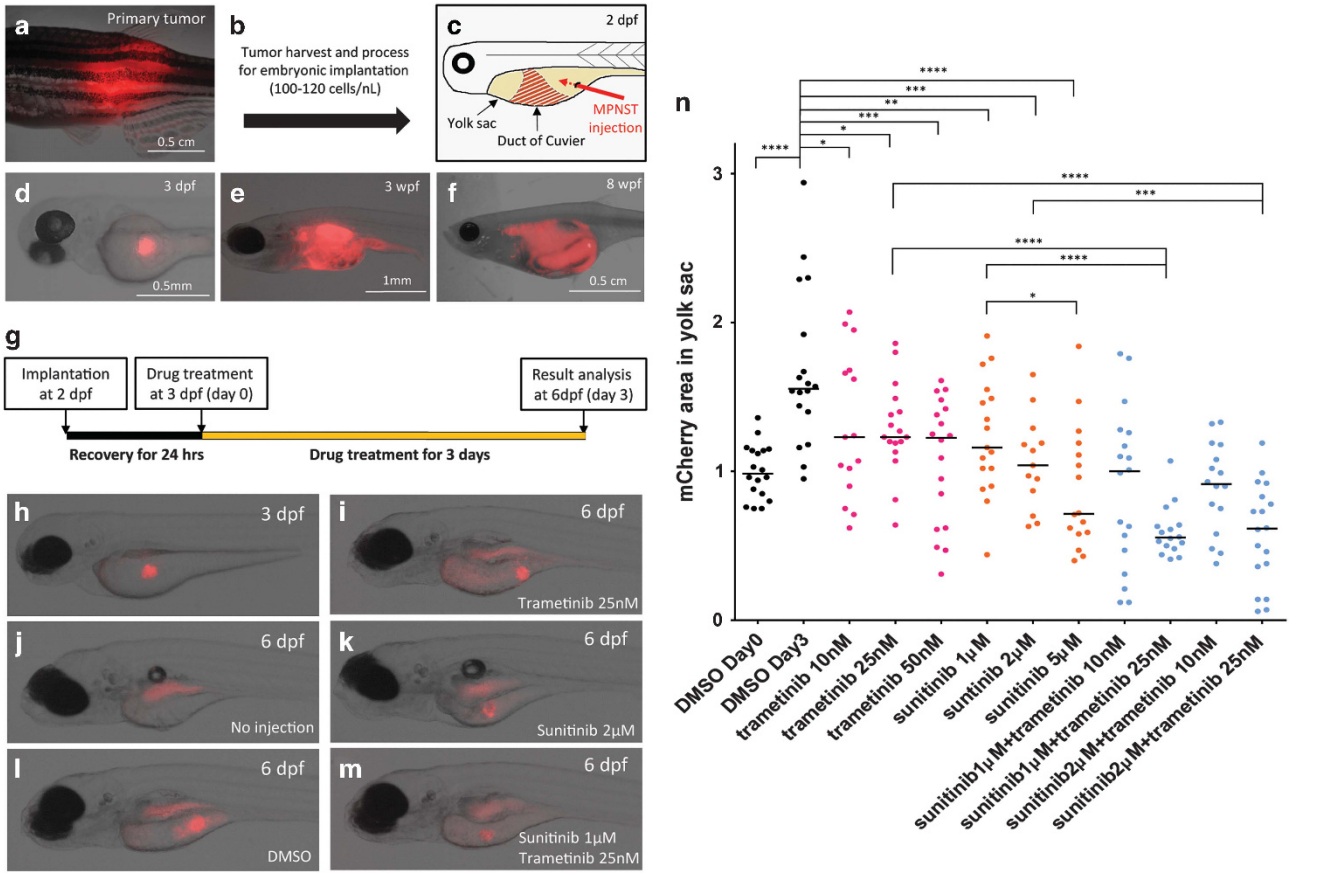

Figure 7. Sunitinib activity is enhanced when given in combination with the MEK inhibitor trametinib in an assay using implanted zebrafish MPNST cells. (**a–f**) Photomicrographs of mCherry expressing transplanted MPNST cells. (**a**) Primary zebrafish MPNSTs were harvested from wild-type *PDGFRA* transgenic fish, and (**b**) ~100–120 tumor cells were implanted into the yolk sac of a 2 d.p.f. embryo. (**c**) Illustration of our implantation. Red arrow represents direction of the microneedle for cell injection. (**d**) Representative image of implanted MPNST embryo at 3 d.p.f. (**e**) Injected MPNST cells were expanded and (**f**) formed tumor mass in embryos. (**g**) Schematic diagram of our implantation and drug treatment assay. MPNST cells were transplanted into 2 d.p.f. embryos and treated with drugs in the fish water from 3 to 6 d.p.f. (**h–m**) Representative fish images at 6 d.p.f. after drug treatment. Because autofluorescence was expressed from the embryo gut (**j**), mCherry expressed areas in yolk sac were only analyzed for this assay. (**n**) MPNST tumor cell growth in the yolk sac of the implanted embryos. These embryos were treated with vehicle control, trametinib, sunitinib or combinations of trametinib and sunitinib ($n = 20$ per condition). The asterisks indicate the range of the different *P*-values of Student's *t*-test (*$P < 0.05$; **$P < 0.01$; ***$P < 0.001$; ****$P < 0.0001$). Black bar in each column scatter plot represents the median value.

(Shin *et al.*[22] and Figures 3g–i) and fluorescent protein driven by the *sox10* promoter is readily apparent in the primary MPNSTs of adult fish under the fluorescent microscope (Figures 2c–h), providing a useful marker for monitoring MPNST growth in living adult tumor bearing fish.

The constitutively active form of *PDGFRA* that we used for this study was first identified in human high-grade gliomas,[23] and possesses an in-frame deletion (exons 8 and 9) in the extracellular domain. We previously reported two cases of high-grade gliomas in the *nf1a*$^{+/-}$; *nf1b*$^{-/-}$; *p53*$^{m/m}$-stable zebrafish line, and these tumor cells expressed Sox10.[22] In our current study, we identified one high-grade glioma in a fish transgenic for the *sox10:PDGFRA mutant* (Supplementary Figure S3), but we did not observe accelerated onset or increased penetrance of high-grade gliomas in the *PDGFRA* transgenic zebrafish. We are not sure why this promoter–receptor combination was not active in promoting the pathogenesis of high-grade gliomas in the zebrafish model. The *sox10-mCherry* expression is clearly visible in the brains of the transgenic fish, but it is possible that the *sox10* promoter is not expressed early enough in the central nervous system glial lineage to drive the transformation of glial stem and progenitor cells. Alternatively, the central nervous system glial cells may be more susceptible to cell senescence induced by the *PDGFRA* transgenes, although we do not observe increased β-gal staining in the central nervous system of these fish.

In a previous study, *PDGFRA* was expressed in 75% of human primary MPNSTs and MPNST cell lines,[16] and overexpression of epidermal growth factor receptor together with *p53* or *pten* mutations increased MPNST development in mouse models.[43,44] Our study supports the hypothesis that wild-type *PDGFRA* overexpression accelerates the onset of MPNST development and would be sensitive to inhibition in MPNST patients. In human MPNSTs, Zietsch *et al.*[13] reported that the cell line S462 harbors the 4q12 amplicon (*PDGFRA*, *KIT* and *KDR* genes) and is sensitive to sunitinib, with an IC50 (half-maximal inhibitory concentration) below 1.0 μM. Moreover, sunitinib induced apoptosis and prevented PDGFRA downstream signaling in response to the ligand, PDGF-AA. Holtkamp *et al.*[16] also reported that PDGFRA in the S462 cell line is phosphorylated in response PDGF-AA. In addition, Aoki *et al.*[19] has shown that cell invasion by the human MPNST cell lines, FU-SFT8611 and FU-SFT9817, is increased in response to the PDGF-AA and PDGF-BB ligands. Based on these results, we believe the role of PDGFRA in MPNST growth is evolutionarily conserved and that our zebrafish model faithfully represents human MPNSTs. Our results showing measurable activities of sunitinib and trametinib appear to accurately reflect the sensitivity of the

human disease. In future studies with our MPNST model, it will be important to test other RTK inhibitors such as imatinib, pazopanib and sorafenib. The ideal properties of the zebrafish system for evaluating the activity of drugs administered into the fish water or delivered by daily oral gavage suggest that this system may be ideal for identifying drugs that can synergize with sunitinib to yield much more substantial levels of tumor cell killing. For example, others have reported activity of MEK[28] and BET[45] inhibitors in human MPNSTs and further investigation revealed that the MEK inhibitor trametinib enhanced antitumor effects of sunitinib *in vivo* (see Figure 7). Assays in the zebrafish may be one of the best ways to test combinations of three or more drugs *in vivo* at multiple dose levels in preclinical studies to guide the development of clinical trials for this disease.

MATERIALS AND METHODS

Zebrafish lines

The *nf1a*$^{+/-}$*; nf1b*$^{-/-}$*; p53*$^{m/m}$ zebrafish line[22] was used for injections to generate the *sox10:PDGFRA* wild-type and mutant and *sox10:mCherry* transgenic lines. Zebrafish were maintained under standard conditions as described previously.[46] All experiments involving zebrafish were approved by the Institutional Animal Care and Use Committee of the Dana-Farber Cancer Institute.

DNA constructs for transgenesis

The 7 kb promoter region of the *sox10* gene was amplified by PCR from a zebrafish promoter construct kindly provided by Dr Robert N Kelsh,[25] and subcloned into vectors to drive the expression of several genes, including *Tg*(*sox10:mCherry*), *Tg*(*sox10:PDGFRA* wild-type) and *Tg*(*sox10:PDGFRA* mutant) in tissues normally expressing the *sox10* gene. The wild-type and mutant *PDGFRA* cDNAs were provided by Dr Eric C Holland.[47] Embryos were injected with these DNA constructs at the one-cell stage and grown to adulthood. Fin clips from the offspring were genotyped for the stable integration and germline transmission of the transgenes. The *Tg*(*sox10:mCherry*), *Tg*(*sox10:PDGFRA* wild-type) and *Tg*(*sox10:PDGFRA* mutant) zebrafish lines are designated the 'mCherry', 'wild-type *PDGFRA*' and '*PDGFRA* mutant' transgenic line in this article, respectively.

Genotyping assays

To extract genomic DNA, embryos or tail clips were placed in clean PCR tubes and 40 µl of lysis buffer (10 mM Tris (pH 8.3), 50 mM KCl, 0.3% Tween-20, 0.3% NP40, 1 mg/ml proteinase K) was added to each tube. The PCR tubes incubated at 55 °C for 2 h to overnight, depending on the size of the sample, and then the tubes were heated to 95 °C for 15 min for the proteinase K inactivation. Using 2 µl of the lysate as a PCR template, PCR reaction was performed with NEB *Taq* DNA polymerase (NEB, Ipswich, MA, USA; M0273) according to the manufacturer's instructions. The primers used for human *PDGFRA* amplification were as follows: (forward) 5′-ATCAAACCCACCTTCAGCCA-3′ and (reverse) 5′-TCAATGACCCTCCAGCGAAT-3′. PCR was started at 95 °C for 2 min and then underwent 40 cycles of 95 °C for 30 s, 55 °C for 30 s and 68 °C for 45 s. For *nf1a, nf1b* and *p53*, we used protocols described previously.[20,22,48]

Tumor watch of transgenic fish

mCherry, wild-type and mutant *PDGFRA* heterozygous transgenic fish were crossed with *nf1a*$^{+/-}$*; nf1b*$^{-/-}$*; p53*$^{m/m}$, and offsprings were screened every week starting from 12 w.p.f. for fluorescent mCherry-expressing cell masses indicative of tumors. In addition, for Figure 2a, either human wild-type or mutant *PDGFRAs* were overexpressed in *nf1*- and *p53*-deficient fish as mosaics by coinjecting the following constructs into the one-cell stage of *nf1*- and *p53*-deficient embryos: (1) *sox10:PDGFRA* wild-type with *sox10:mCherry*; (2) *sox10:PDGFRA* mutant with *sox10:mCherry*; or (3) *sox10:mCherry* alone. The primary injectants were raised and monitored for the onset of tumorigenesis as described above. Fish with tumors were separated and analyzed further by H&E staining and immunohistochemical assays.

Western blotting

Protein lysates were prepared with mCherry expressed tumors from *nf1a*$^{+/-}$*; nf1b*$^{-/-}$*; p53*$^{m/m}$ fish. Briefly, mCherry-positive tumor mass were harvested from tricaine-anesthetized tumor fish, and were lysed on ice in 1× RIPA (Cell Signaling, Danvers, MA, USA) containing, PhosSTOP phosphatase inhibitor cocktail tablet (Roche, Indianapolis, IN, USA) and complete protease inhibitor tablet (Roche). The inhibitors were prepared following the manufacturer's recommendation. Protein lysates were separated by gel electrophoresis, transferred to PVDF membranes and probed overnight at 4 °C with the following primary antibodies: anti-PDGFRA (Cell Signaling; 5241; 1:500), anti-p-tyrosine (EMD Millipore, Billerica, MA, USA; 05-321; 1:1000), anti-β-tubulin (Cell Signaling 2146; 1:2000), anti-AKT (Cell Signaling; 9272; 1:1000), anti-p-AKT (Cell Signaling; 4060; 1:1000), anti-p-ERK1/2 (Cell Signaling; 4377;1:1000) and anti-ERK1/2 (Cell Signaling; 9102; 1:1000). Primary antibody binding was visualized on X-ray film using anti-mouse-HRP (Cell Signaling; 7076; 1:10 000) or anti-rabbit-HRP (Cell Signaling; 7074; 1:10 000) secondary antibodies along with SuperSignal West Dura or Femto (Thermo Fisher Scientific, Waltham, MA, USA) chemiluminescent substrates. Stripping was performed using Restore PLUS Western Blot Stripping Buffer (Thermo Fisher Scientific) according to the manufacturer's protocol.

Senescence-associated β-galactosidase staining

The Senescence-Associated β-Galactosidase Detection Kit (CS0030; Sigma-Aldrich, St Louis, MO, USA) was used for fish embryo senescence detection according to the manufacturer's protocol. Briefly, fish embryos at 4 d.p.f. were fixed with 4% paraformaldehyde for 24 h at 4 °C, and were washed three times in phosphate-buffered saline (pH 7.4) for 1 h each. After washing, the embryos were incubated with the senescence staining mixture for 24 h at 37 °C. The experiment was performed in duplicate.

Paraffin sectioning, cryosectioning and immunostaining

Fish were fixed with 4% paraformaldehyde and embedded in paraffin blocks for paraffin sectioning. Sections were immunostained by conventional protocols[49] using antibodies against S100 (Dako, Carpinteria, CA, USA; Z0311; 1:1000), Sox10 (GeneTex, Irvine, CA, USA; GTX128374; 1:1000), proliferating cell nuclear antigen (EMD Millipore; NA03; 1:50) and cleaved caspase-3 (Cell Signaling 9664; 1:125). Cryosectioning of β-galactosidase-stained embryos was performed as described previously.[50]

Drug treatment

Wild-type *PDGFRA* expressed tumor fish were exposed to 2 µM sunitinib (LC Laboratories, Woburn, MA, USA; S-8803) or DMSO added to the fish water. The tumor fish were fed with dry food (GEMMA Micro 300; Skretting, Tooele, UT, USA) every other day. The fish water was exchanged with fresh water (containing sunitinib or DMSO) 2 h after feeding. After 10 days of treatment, quantitative assessment of the remaining tumor was measured using the ImageJ software (NIH, Bethesda, MD, USA) for each treated tumor fish. Embryos were treated with sunitinib, trametinib (Selleck, Houston, TX, USA; GSK1120212) or a combination of both for 3 days under dark conditions.

Embryonic implantation assay

Primary MPNST cells derived from wild-type *PDGFRA* expressed tumor fish were injected into the yolk sac of each embryo (*roy* and *nacre* double homozygous mutant; casper line) at 2 d.p.f. Successfully implanted embryos were collected and randomly distributed into the well of a 12-well plate, and incubated with either DMSO or drugs for 3 days at 28 °C. After drug treatment for 3 days, each embryo was imaged, and tumor area was quantitated using the ImageJ software (NIH). For further details about the implantation, see Supplementary Information.

Statistical analysis

Statistical analysis was performed with Prism 5 software (GraphPad, La Jolla, CA, USA). Kaplan–Meier methods and the log-rank test were applied to assess the rate of tumor development in Figure 2. The exact sample size is indicated in each figure and legend. A two-tailed unpaired *t*-test was used for the analysis in Figure 4 and data were plotted along with the standard deviation. A two-tailed unpaired *t*-test was also used for the analysis in Figure 5. For the experiment shown in Figure 7, the power to detect a 50% decrease in tumor cells with an agent compared with DMSO

is 91% when nine embryos are tested per condition, assuming that if the mean signal is reduced by 50%, the standard deviation is also reduced by 50%, so at least nine embryos were tested at each condition. The largest and smallest values for each condition were removed from analysis as outliers according to the pre-established criteria, and the median values are shown in Figure 7. A two-tailed unpaired *t*-test was used for the analysis of significance in Figure 7. After drug treatment, digital images were recorded of the fluorescence signal for every embryo and the area of the fluorescence signal was measured quantitatively using the ImageJ software (NIH). The variance of the area of mCherry expression in the embryos was calculated for each group and shown to be within 30% of the DMSO control embryos. If the standard deviation for specific compounds varies by $>30\%$ from the DMSO control embryos, and then we would test for significance using the Welch *t*-test. Embryos were injected without randomization for this experiment. The investigators were not blinded to the experimental group.

CONFLICT OF INTEREST

The authors declare no conflict of interest.

ACKNOWLEDGEMENTS

This work was supported by the Latsis family fellowship from the Boston Children's Hospital Neurofibromatosis program, a grant from Department of Defense (W81XWH-12-1-0125), a Drug Discovery Initiative Award from the Children's Tumor Foundation and the NF1 Research Consortium Fund. We thank John Gilbert for editorial review and critical comments, and Dr Donna Neuberg for biostatistical advice regarding the sample size, statistical power and most appropriate statistical tests. We are grateful to Hillary Layden and Shawna Chamberlin for their expert assistance with zebrafish husbandry and to Dr Eric Holland for providing the wild-type and mutant PDGFRA cDNAs.

AUTHOR CONTRIBUTIONS

DHK, SH and ATL conceived and designed the experiments; DHK performed the experiments; SR performed and analyzed the histologic analysis and immunostaining; DHK, SH and ATL analyzed the data and wrote the paper.

REFERENCES

1 Ferrari A, Bisogno G, Carli M. Management of childhood malignant peripheral nerve sheath tumor. *Paediatr Drugs* 2007; **9**: 239–248.
2 Evans DG, O'Hara C, Wilding A, Ingham SL, Howard E, Dawson J *et al.* Mortality in neurofibromatosis 1: in North West England: an assessment of actuarial survival in a region of the UK since 1989. *Eur J Hum Genet* 2011; **19**: 1187–1191.
3 Thway K, Fisher C. Malignant peripheral nerve sheath tumor: pathology and genetics. *Ann Diagn Pathol* 2013; **18**: 109–116.
4 Kourea HP, Bilsky MH, Leung DH, Lewis JJ, Woodruff JM. Subdiaphragmatic and intrathoracic paraspinal malignant peripheral nerve sheath tumors: a clinicopathologic study of 25 patients and 26 tumors. *Cancer* 1998; **82**: 2191–2203.
5 Wong WW, Hirose T, Scheithauer BW, Schild SE, Gunderson LL. Malignant peripheral nerve sheath tumor: analysis of treatment outcome. *Int J Radiat Oncol Biol Phys* 1998; **42**: 351–360.
6 Cichowski K, Jacks T. NF1 tumor suppressor gene function: narrowing the GAP. *Cell* 2001; **104**: 593–604.
7 Martin GA, Viskochil D, Bollag G, McCabe PC, Crosier WJ, Haubruck H *et al.* The GAP-related domain of the neurofibromatosis type 1 gene product interacts with ras p21. *Cell* 1990; **63**: 843–849.
8 Knudson AG. Two genetic hits (more or less) to cancer. *Nat Rev Cancer* 2001; **1**: 157–162.
9 Rubin JB, Gutmann DH. Neurofibromatosis type 1—a model for nervous system tumour formation? *Nat Rev Cancer* 2005; **5**: 557–564.
10 Fortman BJ, Kuszyk BS, Urban BA, Fishman EK. Neurofibromatosis type 1: a diagnostic mimicker at CT. *Radiographics* 2001; **21**: 601–612.
11 Mautner VF, Friedrich RE, von Deimling A, Hagel C, Korf B, Knofel MT *et al.* Malignant peripheral nerve sheath tumours in neurofibromatosis type 1: MRI supports the diagnosis of malignant plexiform neurofibroma. *Neuroradiology* 2003; **45**: 618–625.
12 Lee W, Teckie S, Wiesner T, Ran L, Prieto Granada CN, Lin M *et al.* PRC2 is recurrently inactivated through EED or SUZ12 loss in malignant peripheral nerve sheath tumors. *Nat Genet* 2014; **46**: 1227–1232.
13 Zietsch J, Ziegenhagen N, Heppner FL, Reuss D, von Deimling A, Holtkamp N. The 4q12 amplicon in malignant peripheral nerve sheath tumors: consequences on gene expression and implications for sunitinib treatment. *PLoS One* 2010; **5**: e11858.
14 Mantripragada KK, Spurlock G, Kluwe L, Chuzhanova N, Ferner RE, Frayling IM *et al.* High-resolution DNA copy number profiling of malignant peripheral nerve sheath tumors using targeted microarray-based comparative genomic hybridization. *Clin Cancer Res* 2008; **14**: 1015–1024.
15 Holtkamp N, Mautner VF, Friedrich RE, Harder A, Hartmann C, Theallier-Janko A *et al.* Differentially expressed genes in neurofibromatosis 1-associated neurofibromas and malignant peripheral nerve sheath tumors. *Acta Neuropathol* 2004; **107**: 159–168.
16 Holtkamp N, Okuducu AF, Mucha J, Afanasieva A, Hartmann C, Atallah I *et al.* Mutation and expression of PDGFRA and KIT in malignant peripheral nerve sheath tumors, and its implications for imatinib sensitivity. *Carcinogenesis* 2006; **27**: 664–671.
17 Perrone F, Da Riva L, Orsenigo M, Losa M, Jocolle G, Millefanti C *et al.* PDGFRA, PDGFRB, EGFR, and downstream signaling activation in malignant peripheral nerve sheath tumor. *Neuro-oncology* 2009; **11**: 725–736.
18 Mashour GA, Ratner N, Khan GA, Wang HL, Martuza RL, Kurtz A. The angiogenic factor midkine is aberrantly expressed in NF1-deficient Schwann cells and is a mitogen for neurofibroma-derived cells. *Oncogene* 2001; **20**: 97–105.
19 Aoki M, Nabeshima K, Koga K, Hamasaki M, Suzumiya J, Tamura K *et al.* Imatinib mesylate inhibits cell invasion of malignant peripheral nerve sheath tumor induced by platelet-derived growth factor-BB. *Lab Invest* 2007; **87**: 767–779.
20 Berghmans S, Murphey RD, Wienholds E, Neuberg D, Kutok JL, Fletcher CD *et al.* Tp53 mutant zebrafish develop malignant peripheral nerve sheath tumors. *Proc Natl Acad Sci USA* 2005; **102**: 407–412.
21 Legius E, Dierick H, Wu R, Hall BK, Marynen P, Cassiman JJ *et al.* TP53 mutations are frequent in malignant NF1 tumors. *Genes Chromosomes Cancer* 1994; **10**: 250–255.
22 Shin J, Padmanabhan A, de Groh ED, Lee JS, Haidar S, Dahlberg S *et al.* Zebrafish neurofibromatosis type 1 genes have redundant functions in tumorigenesis and embryonic development. *Dis Models Mech* 2012; **5**: 881–894.
23 Clarke ID, Dirks PB. A human brain tumor-derived PDGFR-alpha deletion mutant is transforming. *Oncogene* 2003; **22**: 722–733.
24 Langenau DM, Keefe MD, Storer NY, Jette CA, Smith AC, Ceol CJ *et al.* Co-injection strategies to modify radiation sensitivity and tumor initiation in transgenic Zebrafish. *Oncogene* 2008; **27**: 4242–4248.
25 Dutton JR, Antonellis A, Carney TJ, Rodrigues FS, Pavan WJ, Ward A *et al.* An evolutionarily conserved intronic region controls the spatiotemporal expression of the transcription factor Sox10. *BMC Dev Biol* 2008; **8**: 105.
26 Nonaka D, Chiriboga L, Rubin BP. Sox10: a pan-schwannian and melanocytic marker. *Am J Surg Pathol* 2008; **32**: 1291–1298.
27 Karamchandani JR, Nielsen TO, van de Rijn M, West RB. Sox10 and S100 in the diagnosis of soft-tissue neoplasms. *Appl Immunohistochem Mol Morphol* 2012; **20**: 445–450.
28 Jessen WJ, Miller SJ, Jousma E, Wu J, Rizvi TA, Brundage ME *et al.* MEK inhibition exhibits efficacy in human and mouse neurofibromatosis tumors. *J Clin Invest* 2013; **123**: 340–347.
29 Toffalini F, Demoulin JB. New insights into the mechanisms of hematopoietic cell transformation by activated receptor tyrosine kinases. *Blood* 2010; **116**: 2429–2437.
30 Corless CL, Schroeder A, Griffith D, Town A, McGreevey L, Harrell P *et al.* PDGFRA mutations in gastrointestinal stromal tumors: frequency, spectrum and *in vitro* sensitivity to imatinib. *J Clin Oncol* 2005; **23**: 5357–5364.
31 Demoulin JB, Montano-Almendras CP. Platelet-derived growth factors and their receptors in normal and malignant hematopoiesis. *Am J Blood Res* 2012; **2**: 44–56.
32 Medves S, Demoulin JB. Tyrosine kinase gene fusions in cancer: translating mechanisms into targeted therapies. *J Cell Mol Med* 2012; **16**: 237–248.
33 Cools J, DeAngelo DJ, Gotlib J, Stover EH, Legare RD, Cortes J *et al.* A tyrosine kinase created by fusion of the PDGFRA and FIP1L1 genes as a therapeutic target of imatinib in idiopathic hypereosinophilic syndrome. *N Engl J Med* 2003; **348**: 1201–1214.
34 Verhaak RG, Hoadley KA, Purdom E, Wang V, Qi Y, Wilkerson MD *et al.* Integrated genomic analysis identifies clinically relevant subtypes of glioblastoma characterized by abnormalities in PDGFRA, IDH1, EGFR, and NF1. *Cancer Cell* 2010; **17**: 98–110.
35 Velghe AI, Van Cauwenberghe S, Polyansky AA, Chand D, Montano-Almendras CP, Charni S *et al.* PDGFRA alterations in cancer: characterization of a gain-of-function V536E transmembrane mutant as well as loss-of-function and passenger mutations. *Oncogene* 2014; **33**: 2568–2576.
36 Serrano M, Lin AW, McCurrach ME, Beach D, Lowe SW. Oncogenic ras provokes premature cell senescence associated with accumulation of p53 and p16INK4a. *Cell* 1997; **88**: 593–602.

37 Dimauro T, David G. Ras-induced senescence and its physiological relevance in cancer. *Curr Cancer Drug Targets* 2010; **10**: 869–876.
38 Downward J. Ras signalling and apoptosis. *Curr Opin Genet Dev* 1998; **8**: 49–54.
39 Baker SA, Hennig GW, Salter AK, Kurahashi M, Ward SM, Sanders KM. Distribution and Ca(2+) signalling of fibroblast-like (PDGFR(+)) cells in the murine gastric fundus. *J Physiol* 2013; **591**: 6193–6208.
40 Alexander A. Endocytosis and intracellular sorting of receptor tyrosine kinases. *Front Biosci* 1998; **3**: d729–d738.
41 Riemenschneider MJ, Mueller W, Betensky RA, Mohapatra G, Louis DN. *In situ* analysis of integrin and growth factor receptor signaling pathways in human glioblastomas suggests overlapping relationships with focal adhesion kinase activation. *Am J Pathol* 2005; **167**: 1379–1387.
42 Britsch S, Goerich DE, Riethmacher D, Peirano RI, Rossner M, Nave KA *et al.* The transcription factor Sox10 is a key regulator of peripheral glial development. *Genes Dev* 2001; **15**: 66–78.
43 Keng VW, Watson AL, Rahrmann EP, Li H, Tschida BR, Moriarity BS *et al.* Conditional inactivation of Pten with EGFR overexpression in schwann cells models sporadic MPNST. *Sarcoma* 2012; **2012**: 620834.
44 Rahrmann EP, Watson AL, Keng VW, Choi K, Moriarity BS, Beckmann DA *et al.* Forward genetic screen for malignant peripheral nerve sheath tumor formation identifies new genes and pathways driving tumorigenesis. *Nat Genet* 2013; **45**: 756–766.
45 De Raedt T, Beert E, Pasmant E, Luscan A, Brems H, Ortonne N *et al.* PRC2 loss amplifies Ras-driven transcription and confers sensitivity to BRD4-based therapies. *Nature* 2014; **514**: 247–251.
46 Westerfield M. *The Zebrafish Book. A Guide for the Laboratory use of Zebrafish (Danio rerio)*4th edn.University of Oregon Press, 2000.
47 Ozawa T, Brennan CW, Wang L, Squatrito M, Sasayama T, Nakada M *et al.* PDGFRA gene rearrangements are frequent genetic events in PDGFRA-amplified glioblastomas. *Genes Dev* 2010; **24**: 2205–2218.
48 Lee JS, Padmanabhan A, Shin J, Zhu S, Guo F, Kanki JP *et al.* Oligodendrocyte progenitor cell numbers and migration are regulated by the zebrafish orthologs of the NF1 tumor suppressor gene. *Hum Mol Genet* 2010; **19**: 4643–4653.
49 Macdonald R. Zebrafish immunohistochemistry. *Methods Mol Biol* 1999; **127**: 77–88.
50 Tao T, Shi H, Guan Y, Huang D, Chen Y, Lane DP *et al.* Def defines a conserved nucleolar pathway that leads p53 to proteasome-independent degradation. *Cell Res* 2013; **23**: 620–634.

Supplementary Information accompanies this paper on the Oncogene website (http://www.nature.com/onc)